Article:

Gardner, RL, Piazolo, S orcid.org/0000-0001-7723-8170, Daczko, NR et al. (1 more author) (2020) Microstructures reveal multistage melt present strain localisation in mid-ocean gabbros. Lithos, 366-367. 105572. ISSN 0024-4937

https://doi.org/10.1016/j.lithos.2020.105572

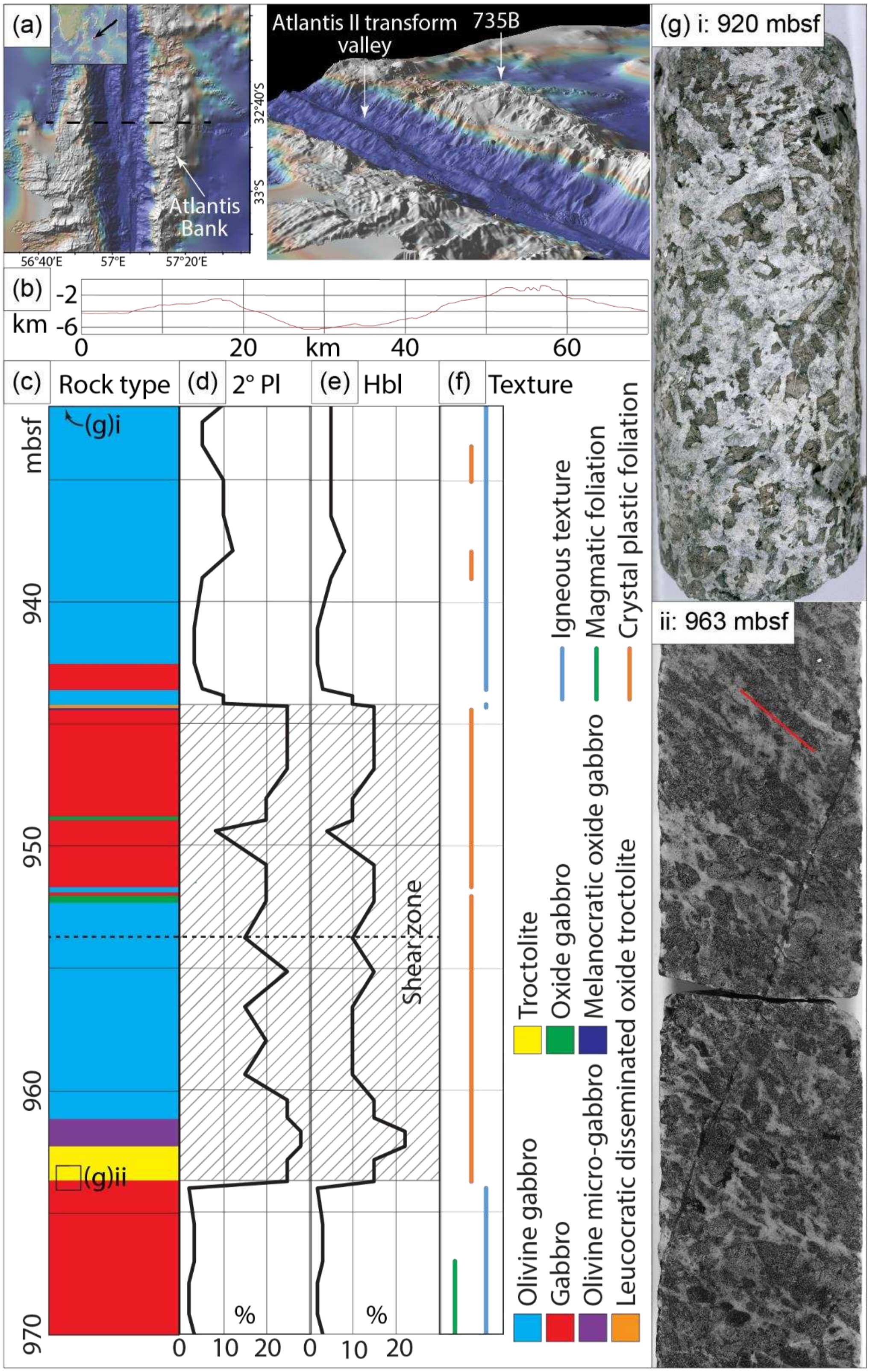

(a)
Atlantis II transform valley
735B
32°40'S
33°S
Atlantis Bank
56°40'E
57°E
57°20'E
(b)
-2
km
-6
0
20
km
40
60
(c)
Rock type
(d)
2° Pl
(e)
Hbl
(f)
Texture
mbsf
940
950
960
970
(g)i
(g)ii
Shear zone
%
0
10
20
Igneous texture
Magmatic foliation
Crystal plastic foliation
Olivine gabbro
Gabbro
Olivine micro-gabbro
Leucocratic disseminated oxide troctolite
Troctolite
Oxide gabbro
Melanocratic oxide gabbro
(g) i: 920 mbsf
ii: 963 mbsf

Figure 1: Geological context of the studied sample; (a) location of Atlantis Bank and core 735B (Ryan et al., 2009), profile for (b) marked; (b) profile across the Atlantis fracture zone and Atlantis Bank showing relative height of the core complex (GMRT Grid Version 3.6); core section (from shipboard core description) showing: (c) dominant rock types, note location of the 20m thick shear zone studied is marked by cross hatching; (d) proportions of secondary plagioclase (2° Pl), recognized as irregularly distributed recrystallisation of primary plagioclase (e) proportions of secondary Hbl, seen as alteration rims on olivine and pyroxene and along pyroxene cleavages; (f) textures and foliations recognized in the core; (g) images (IODP reference for pictures – url: http://web.iodp.tamu.edu/janusweb/imaging/closeup.cgi?reporttype=I&leg=176&site=735&hole=B or via http://web.iodp.tamu.edu/OVERVIEW/?&exp=176&site=735) typical of the core, i) showing magmatic crystallization from 920 metres below seafloor (mbsf), ii) showing a typical core image of the 20m thick shear zone shown in (c) at 963 mbsf; location of studied sample is marked by dashed line at 953.7 mbsf. Note that the whole shown section belongs to base of rock unit X.

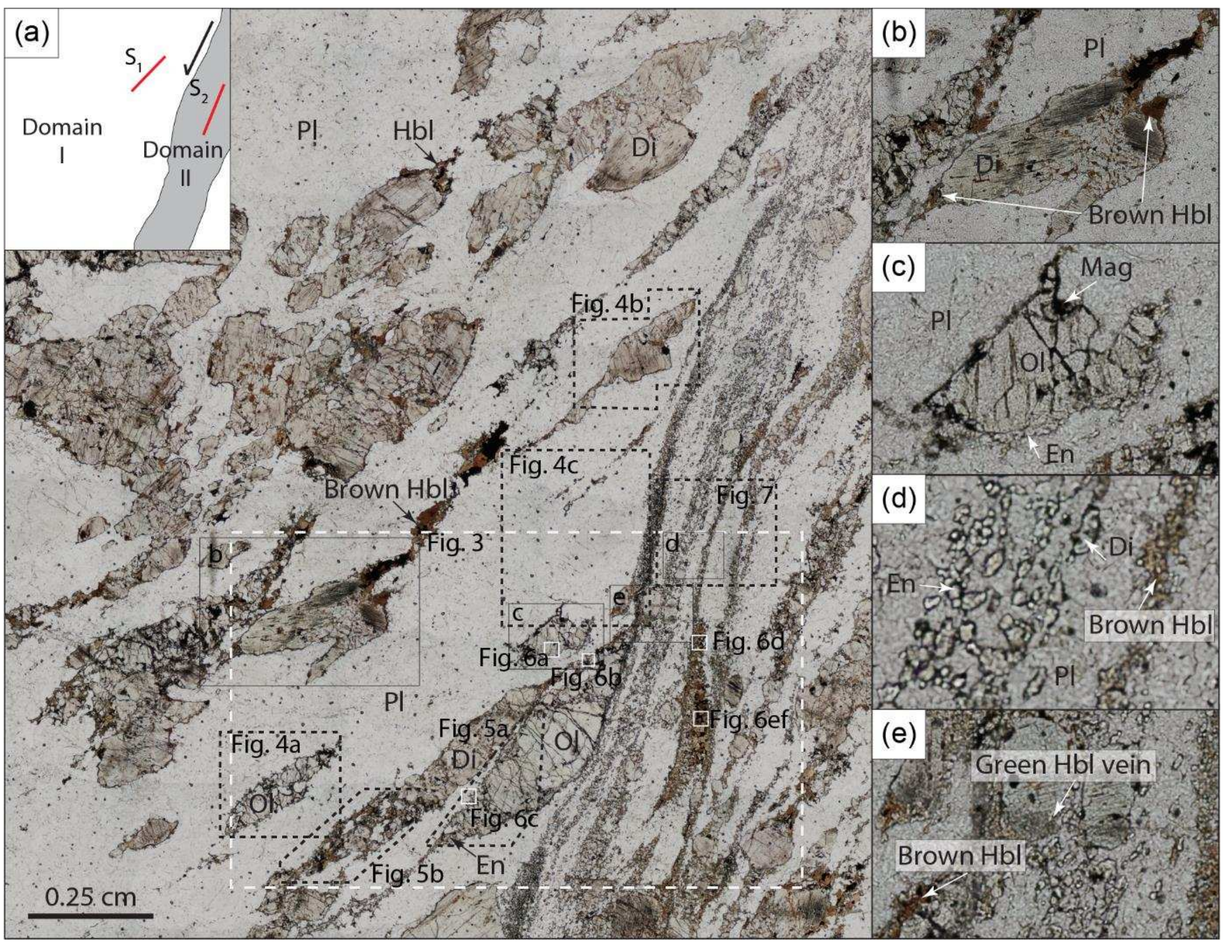

Figure 2. Overview of sample studied depicting main microstructural domains and their characteristics; plane polarized light thin section with locations of other figures white dashed for Synchrotron data, black dotted for EBSD pole figures, solid white for SEM images), solid black for (b) to (e); (insert)

schematic diagram showing domains and foliations; (b) zoom-in showing brown pleochroic hornblende in strain shadows on diopside; (c) zoom-in showing enstatite and magnetite development on edge of olivine; (d) zoom-in showing small grain size and phase mixing of diopside, enstatite, brown pleochroic hornblende and magnetite; (e) zoom-in showing late green pleochroic hornblende vein; mineral abbreviations are following Whitney and Evans (2010).

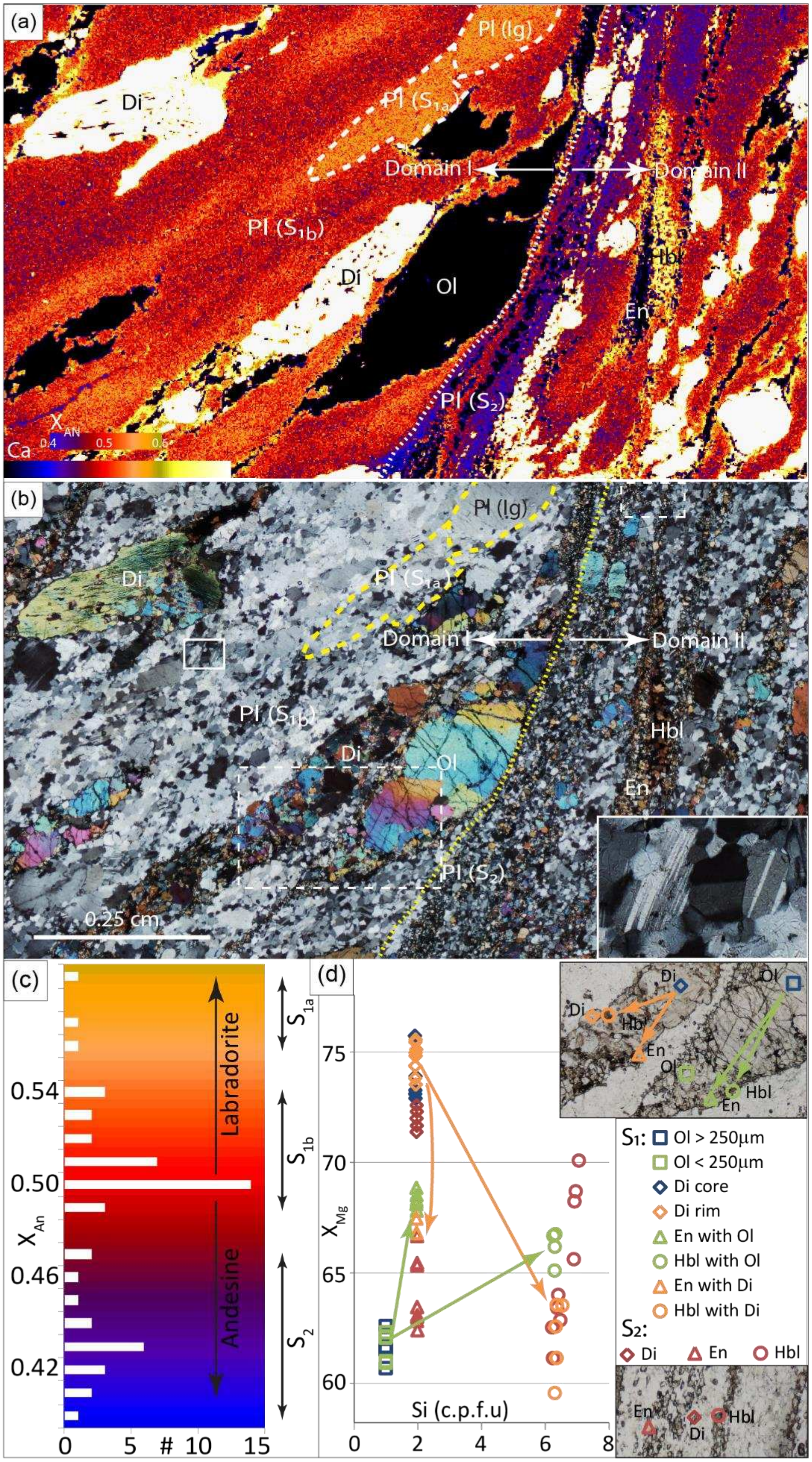
(a)
Di
Pl (lg)
Pl (S_{1a})
Domain I
Domain II
Pl (S_{1b})
Di
Ol
Hbl
En
Pl (S_2)
X_{AN}
Ca
0.4
0.5
0.6
(b)
Pl (lg)
Di
Pl (S_{1a})
Domain I
Domain II
Pl (S_{1b})
Hbl
Di
Ol
En
Pl (S_2)
0.25 cm
(c)
0.54
0.50
X_{An}
0.46
0.42
Labradorite
Andesine
S_{1a}
S_{1b}
S_2
0
5
#
10
15
(d)
X_{Mg}
75
70
65
60
Si (c.p.f.u)
0
2
4
6
8
Di
Ol
Di
Hbl
En
Ol
Hbl
En
S_1: Ol > 250μm
Ol < 250μm
Di core
Di rim
En with Ol
Hbl with Ol
En with Di
Hbl with Di
S_2:
Di
En
Hbl
En
Di
Hbl

Fig 3: Mineral chemistry and its relationship to microstructural features; note all hornblende analyses refer to brown pleochroic hornblende as described in text and Fig. 2 (a) Synchrotron Ca map, equivalent colours for electron microprobe X_{An} calculations are shown; (b) equivalent area from (a) in XPL, showing original igneous (Ig) Pl, Pl recrystallized in S_{1a}, S_{1b} and S_2. Edge of S_2 domain is shown (depicted by yellow dotted line and arrows). Areas of S1a igneous plagioclase and S1b recrystallised plagioclase are outlined in yellow dashed lines. An example of deformation twinning is shown in the zoomed in micrograph (lower right corner; field of view 0.5 mm); (c) plagioclase composition histogram of electron microprobe X_{An} calculations using same key as (a); (d) electron microprobe X_{Mg} calculations for igneous Ol (blue squares) and Di (blue diamonds), S_{1a} recrystallised Ol and Di (green squares and orange diamonds, respectively), S_{1b} reaction products of En and Hbl after Ol (green triangles and circles respectively) and after Di (orange triangles and circles respectively), S_2 reaction products (red symbols); context PPL images (areas in indicated in (b) by white dashed boxes) provided with key; insets show typical locations for each symbol.

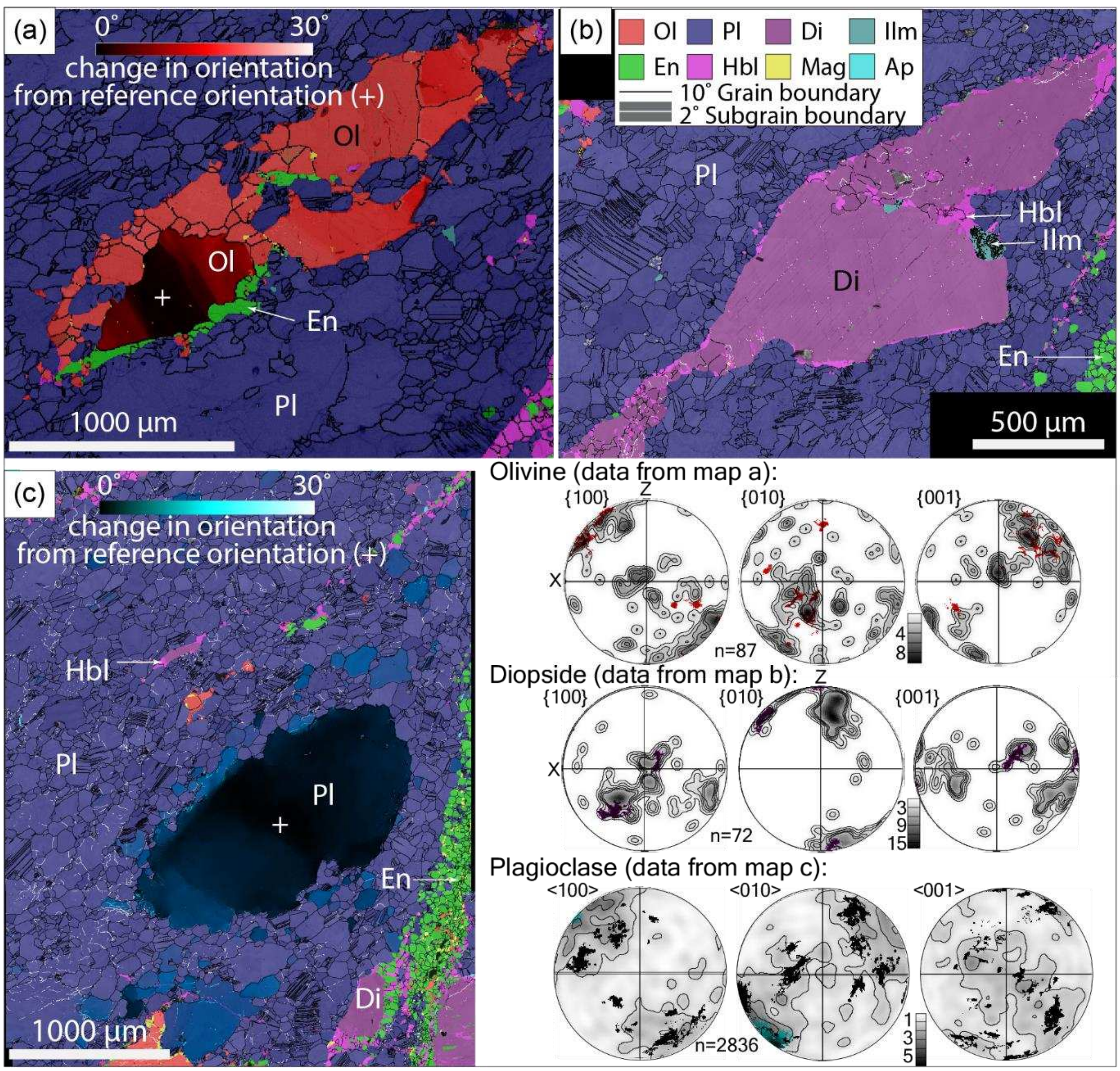

Figure 4: Characteristics of S_{1a} based on EBSD analysis highlighting solid state deformation features such as dynamic recrystallisation of (a) olivine, (b) diopside, (c) plagioclase. 10° grain boundaries marked in black, 2° subgrain boundaries marked in white. Pole figures are grains less than 200 µm diameter, one point per grain in grey shades, overlaid by all points in grains greater than 200 µm diameter marked in the same colour as the map. In (a) for olivine and (c) for plagioclase the change in orientation from a reference orientation (marked with a white cross) is shown.

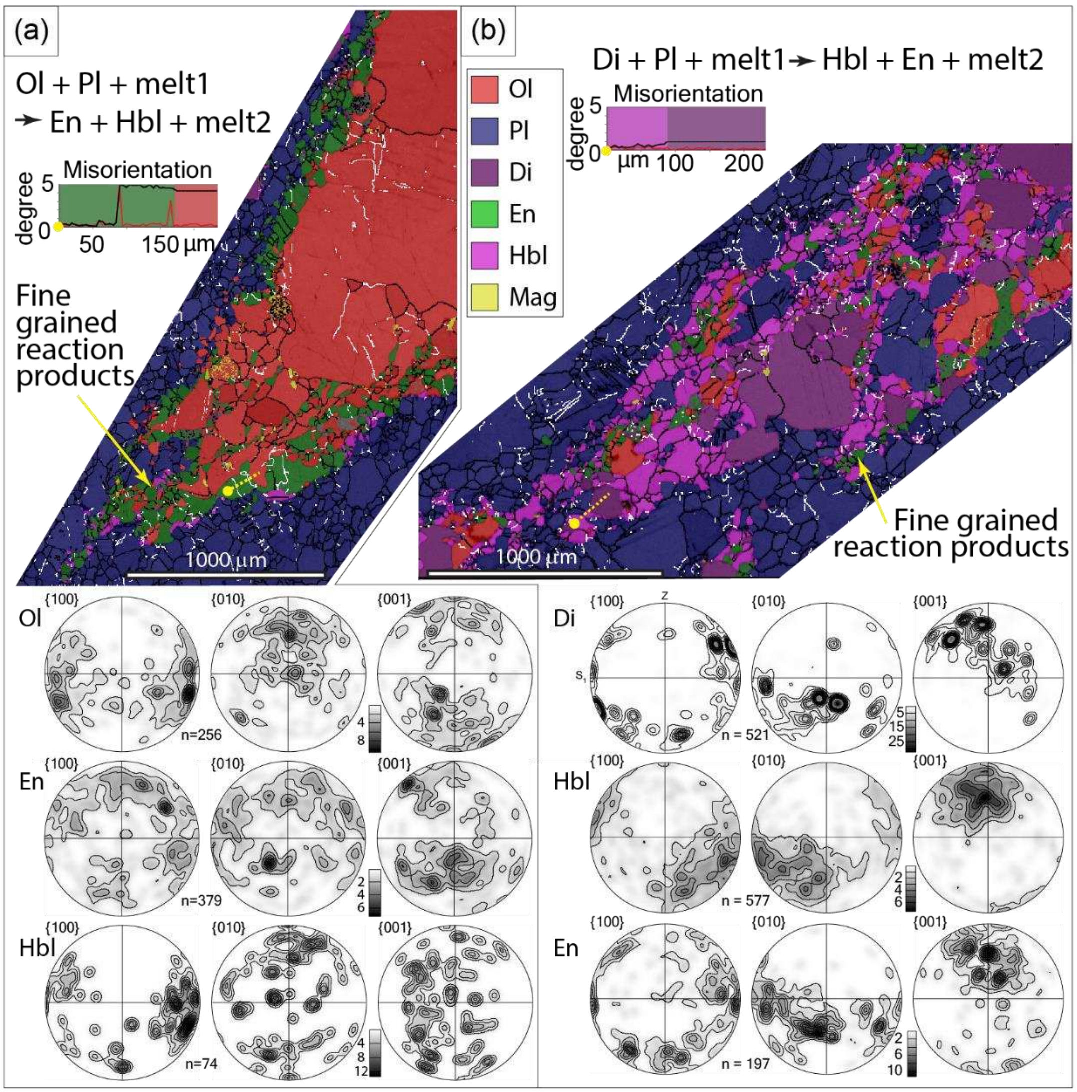

Figure 5. Characteristics of S_{1b} based on EBSD analysis highlighting melt-mineral reactions (a) for Ol, (b) for Di. Misorientation profiles from locations marked with yellow dot and dashed line; background colours show mineral; black lines within profiles depict relative orientation change to the profiles' starting point (marked with yellow dot), red lines depict relative orientation change to the neighbours. Note: En and Hbl reaction products are fine grained and display epitaxy relative to the precursor Igneous or S_{1a} Ol and Di crystallography. All pole figures are 1 point per grain. Colour scheme shown on (a) and (b) are the same as in Figure 4; 10° grain boundaries are black, 2° subgrain boundaries are white.

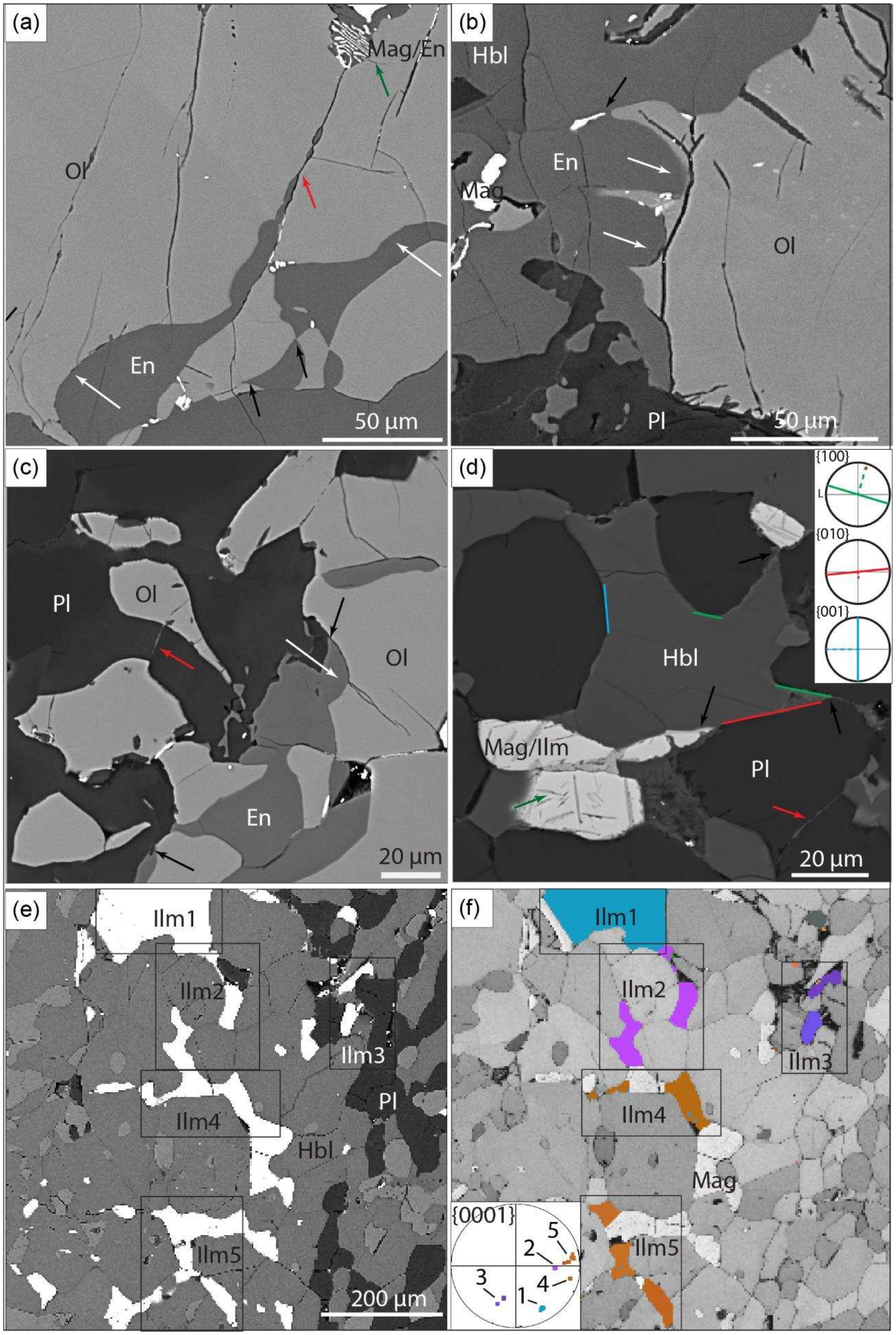
(a)
Mag/En
Ol
En
50 µm
(b)
Hbl
En
Mag
Ol
Pl
50 µm
(c)
Pl
Ol
Ol
En
20 µm
(d)
{100}
L
{010}
{001}
Hbl
Mag/Ilm
Pl
20 µm
(e)
Ilm1
Ilm2
Ilm3
Ilm4
Pl
Hbl
Ilm5
200 µm
(f)
Ilm1
Ilm2
Ilm3
Ilm4
Mag
{0001}
5
2
4
3
1
Ilm5

Figure 6. Melt microstructures; back-scattered electron (BSE) images of S_{1b} and S_2 melt-rock interaction microstructures; (a) to (c) S_{1b}, (d) to (f) S_2. Arrows point to microstructures: red – mineral films along grain boundaries inferred to have pseudomorphed melt, black - low dihedral angles, white – embayments, green - intergrowths. (d) pole figures for central hornblende grain show grain has some crystal faces; note the correlation between colour of crystal planes marked in the pole figure and those in the BSE image. (e) & (f) are the same area of the S_2 domain showing grains connected in 3D (ilmenite grains are numbered Ilm1 to 5, plagioclase grains marked with a red asterisk); ilmenite grains can be differentiated by their orientations (from EBSD data), where the same colour signifies the same crystallographic orientation; colours are repeated on pole figure; data is presented by overlaying EBSD data onto the greyscale EBSD derived band contrast image in (f).

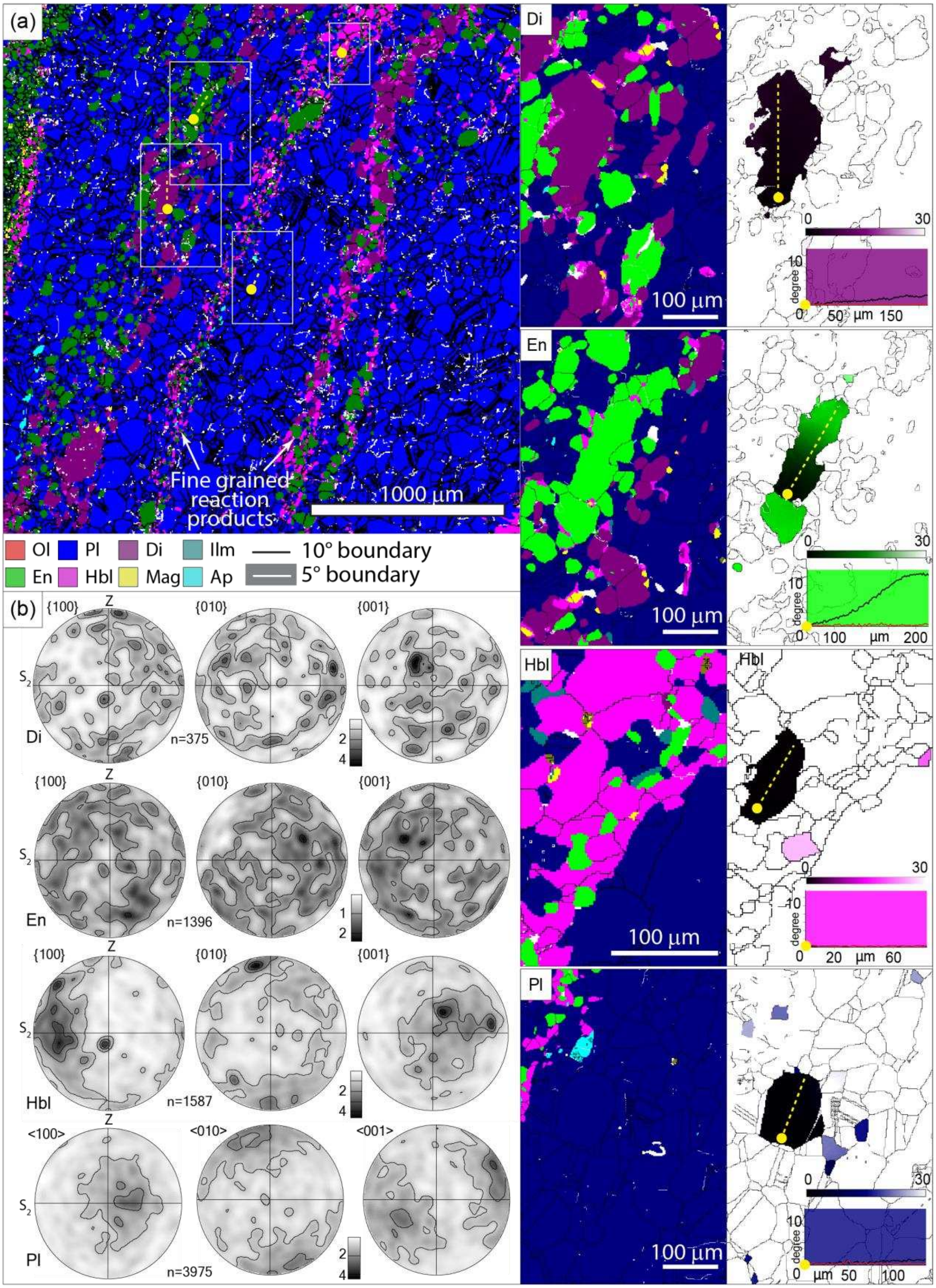

(a)
Fine grained reaction products
1000 μm
Ol Pl Di Ilm 10° boundary
En Hbl Mag Ap 5° boundary
(b)
{100} {010} {001}
Z
S2
Di
n=375
En
n=1396
Hbl
n=1587
<100> <010> <001>
Pl
n=3975
Di
En
Hbl
Pl
100 μm
degree
μm

Figure 7. Characteristics of S_2 based on EBSD analysis highlighting (a) reaction product minerals showing fine grain sizes, and random orientations in (b) pole figures. Misorientation profiles from locations marked with yellow dot and dashed line; background colours show mineral; black lines within profiles depict relative orientation change to the profiles' starting point (marked with yellow dot), red lines depict relative orientation change to the neighbours. Note: all minerals are fine grained with no internal orientation change in diopside, hornblende and plagioclase minerals, while the larger enstatite grains show some orientation change suggesting the latter are residual from S_{1b}; background colours as for mineral colours. Pole figures show all grains in the map area shown with one point per grain plotted. Colour scheme shown on (a) and (b) are the same as in Figure 4; 10° grain boundaries are black, 2° subgrain boundaries are white.

Method	Sx	Min	Max	Median	Reference
Ca in En	S1b	907	1093	1026	B&K 1990
Hbl comp	S1b	863	969	949	Putirka 2016
Hbl comp	S1b	846	961	906	R&R 2012
Ca in En	S2	929	1058	1000	B&K 1990
Hbl comp	S2	869	965	905	Putirka 2016
Hbl comp	S2	753	946	840	R&R 2012
Two Pyx*	S2	798	823	817	B&K 1990*

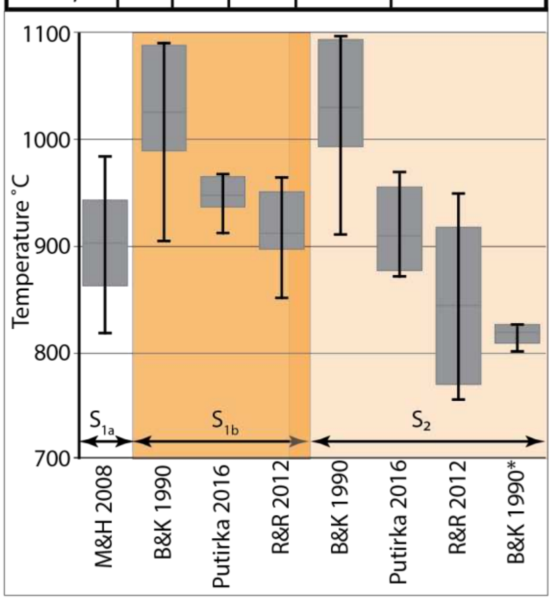

Figure 8. Representative temperatures for deformation of the 735B core. M&H 2008 = Mehl and Hirth (2008), B&K 1990 = Brey and Köhler (1990), Putirika 2016 = Putirika (2016), R&R 2012 = Ridolfi and Renzulli (2012); * indicates Brey and Köhler (1990) two pyroxene thermometer. Note that temperatures for S_{1a} (solid state deformation) are lower than for S_{1b} (820-970˚C) and S_2 (750-900˚C) both of which have melt present. The En and Hbl temperatures reflect that of products from the melt reactions. We interpret this as the matrix temperature gradually reducing, while multiple influxes of hot melt causedg the formation of En and Hbl at shotter than matrix temperatures. Between the melt influxes temperature of the melt gradually equilibrated with the matrix.

(d) Melt present deformation (S_2)	(c) Melt present deformation (S_{1b})	(b) Solid state deformation (S_{1a})	(a) Magmatic foliation (S_0)	
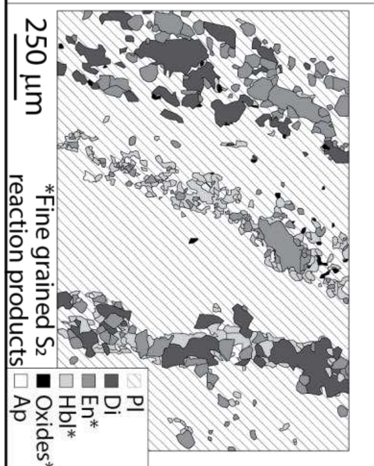	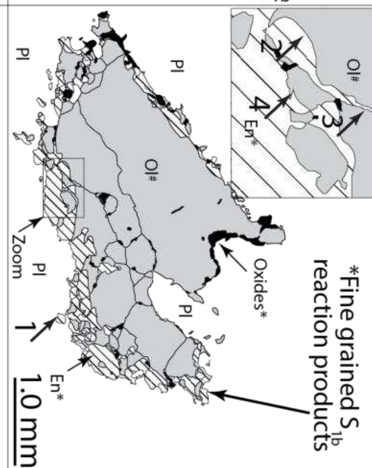	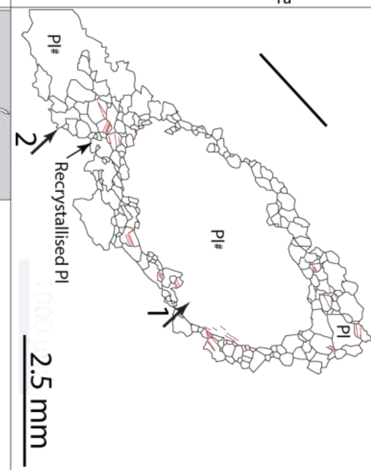	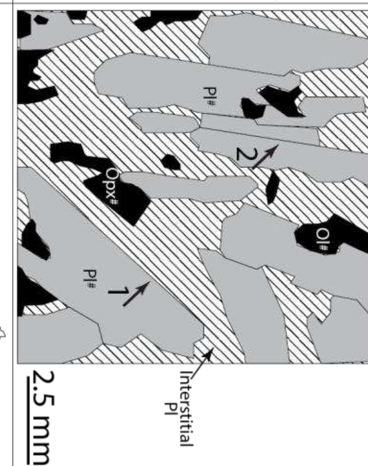	Typical microstructures
Diffusion creep/GBS_melt	Minor dislocation creep/ GBS_melt	Dislocation creep/ local diffusion creep & GBS	NA	Defomration mechanism
High	High	Very low	Low	Degree of open chemical system
GSR_react	GSR_react/GSR_disloc	GSR_disloc	N	Grainsize reduction
Y	Y	N	N	Reaction textures
Y	Y	N	N	Chemical changes
Y	Y	N	N	Assemblage changes
Y	Y	N	Y	Melt presence
Subsequent influx of melt (S_2)	*Initial influx of melt (S_{1b})*	*Solid state deformation (S_{1a})*	*Crystallisation (S_0)*	Timeline

Figure 9. Summary of different deformation environments recorded in the analysed section. (a) S_0: Magmatic foliation showing euhedral grains (1) aligned in the magmatic flow (2); sketch based on micrograph image of Deans and Yoshinobu (2019, Fig.4b). (b) S_{1a}: Solid state deformation showing large porphyroclasts of anhedral plagioclase (1) with fine grained recrystallized plagioclase in strain shadows (2); sketch based on micrography shown in Figure 4c. (c) S_{1b}: Melt present deformation identified by the presence of typical melt present microstructures including asymmetric new mineral growth (1), embayments into original minerals (2), melt films (3) and low dihedral angles of new minerals from the melt (4); note that there is a significant replacement of original S_0 and S_{1a} phases marked by #) by phases associated with melt-rock interaction (En, oxides marked by asterix); sketch based on micrography shown in Figure 3b. (d) S_2: High strain melt present deformation with high melt flux resulting in microstructures typical for melt present deformation as shown in (c) (not shown in sketch), near complete replacement of original S_0 and S_{1a} phases by phases associated with melt-rock interaction (En, Hbl, oxides marked by asterix in legend) and clear phase mixing; see text for details. Abbreviations: GSR_disloc - dislocation creep related grain size reduction, GSR_react – melt reaction related grain size reduction, GBS – grain boundary sliding, GBS_melt melt assisted grain boundary sliding.

Graphical abstract:

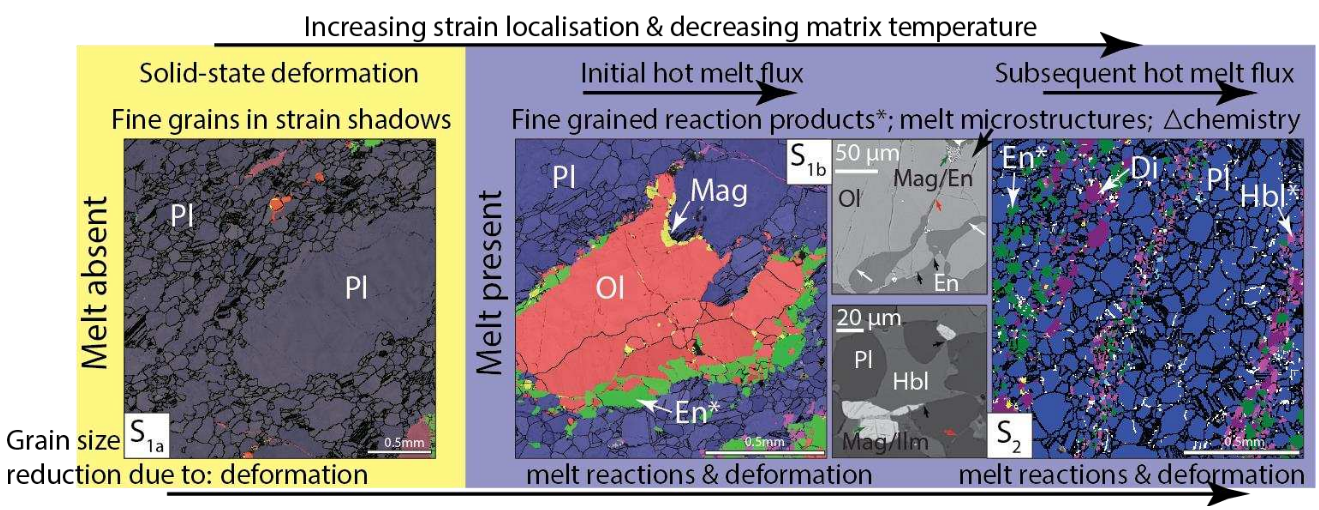

Deans, J. R. L., & Yoshinobu, A. S. (2019). Geographically re-oriented magmatic and metamorphic foliations from ODP Hole 735B Atlantis Bank, Southwest Indian Ridge: Magmatic intrusion and crystal-plastic overprint in the footwall of an oceanic core complex. *Journal of Structural Geology, 126*, 1-10. http://www.sciencedirect.com/science/article/pii/S0191814118305601

Ryan, W. B. F., Carbotte, S. M., Coplan, S., O'Hara, A., Melkonian, A., Arko, R., et al. (2009). Global Multi-Resolution Topography (GMRT) synthesis data set. *Geochemistry, Geophysics, Geosystems, 10*(3).

Whitney, D. L., & Evans, B. W. (2010). Abbreviations for names of rock-forming minerals. *American mineralogist, 95*(1), 185.

Supp figure below…

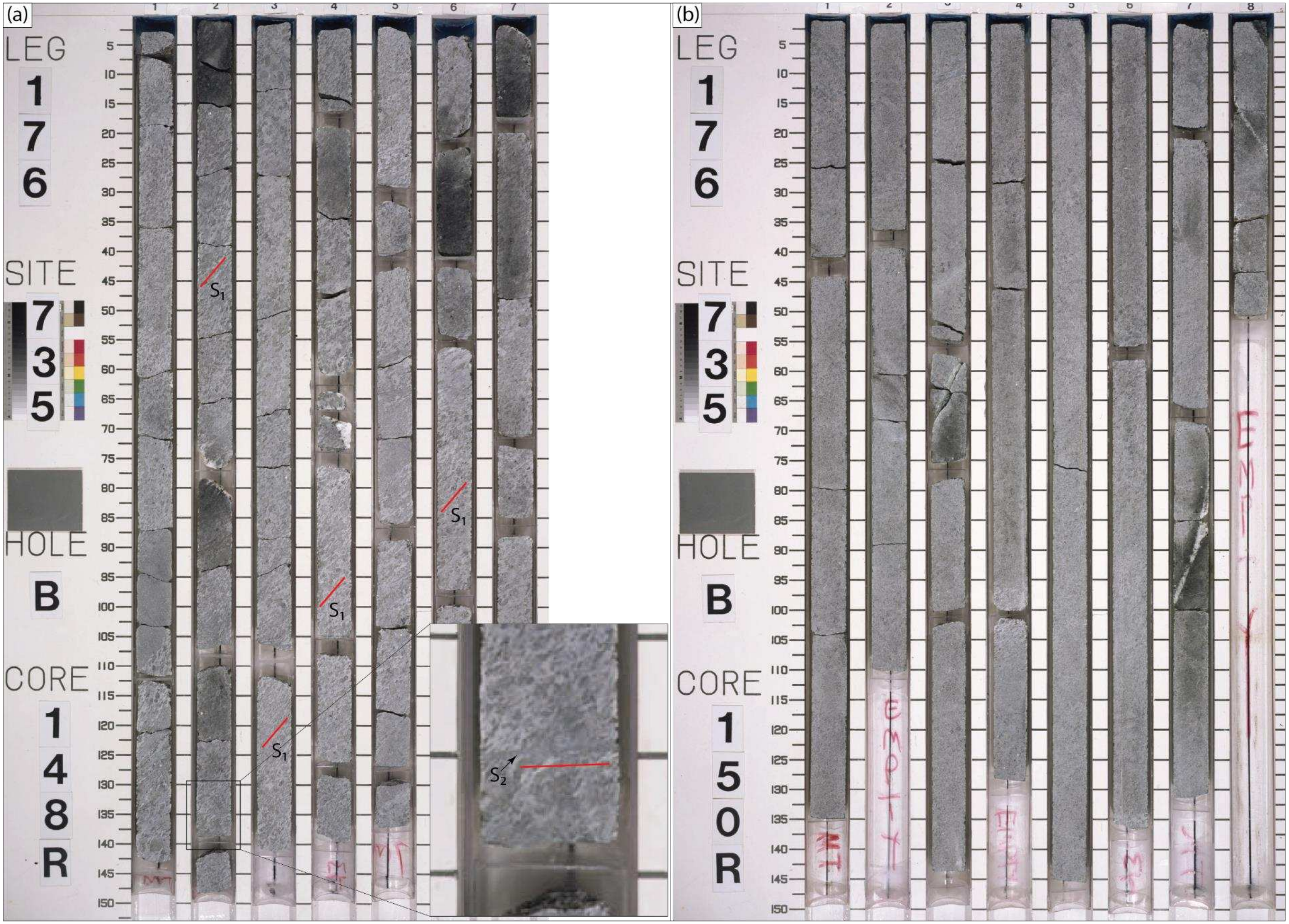
(a)
LEG 1 7 6
SITE 7 3 5
HOLE B
CORE 1 4 8 R
S_1
S_1
S_1
S_1
S_2
MT
(b)
LEG 1 7 6
SITE 7 3 5
HOLE B
CORE 1 5 0 R
MT
EMPTY
EMPTY
EMPTY

Supp Fig 1. Images of the core showing (a) S1 and S2 folitaions in the shear zone, from core 148R (950.9 to 960.5 mbsf) and (b) igneous texture outside the shear zone, from core 150R (979.8 to 987.5 mbsf). Images from

http://www-odp.tamu.edu/publications/176_IR/VOLUME/CORES/IMAGES/735B148R.PDF and

http://www-odp.tamu.edu/publications/176_IR/VOLUME/CORES/IMAGES/735B150R.PDF (23Mar2020)